Influence of the molecular weight of poly(methyl methacrylate) on fracture morphology in notched tension

R. P. Kusy and D. T. Turner
Dental Research Center, University of North Carolina at Chapel Hill, North Carolina 27514, USA
(Received 29 July 1976)

Specimens of poly(methyl methacrylate) (PMMA) were prepared by radiolysis of a polymer from an initial viscosity-average molecular weight ($\bar{M}_v$) of 1.2×10^6 down to 2.6×10^3. At a molecular weight of 1×10^5, abrupt changes in fracture morphology were observed correlating with a similarly abrupt decrease in fracture surface energy (γ). As the molecular weight was decreased further, the fracture morphology resembled more that of very brittle materials such as silicate glasses. Evidence was obtained that Wallner lines can influence the disposition of ribs but not their spacing. An empirical relationship was established between functions of rib spacing (r) and fracture surface energy.

INTRODUCTION

The influence of molecular weight on the fracture morphology of poly(methyl methacrylate) was studied by Newman and Wolock[1] using cast specimens which ranged in viscosity-average molecular weight from 3.2×10^6 to 9×10^4. Specimens were fractured in tension at a constant grip separation of 0.1 cm/min. A decrease in molecular weight was found to result in a decrease in area of the mirror region and in the spacing between ribs. Likewise, conic markings became smaller with decreasing molecular weight and were not observed at all in the specimen of lowest molecular weight. In order to improve optical resolution, Newman and Wolock deposited a thin layer of silver on the fracture surfaces. As a result, no surface colours were described[2,3].

More recently, the trends observed by Newman and Wolock were confirmed and extended in experiments in which an irradiated bar of PMMA, which varied along its length from $\bar{M}_v = 2.2 \times 10^5$ down to $\bar{M}_v = 1.9 \times 10^4$, was fractured by cleavage. In addition the disappearance of surface colours at lower molecular weights and the incidence of relatively featureless regions of glassy fracture were revealed[4].

The purpose of the present paper is to report the fracture morphology of notched specimens of PMMA fractured in tension down to $\bar{M}_v = 2.6 \times 10^3$. The data supplement measurements of fracture surface energy previously reported for similar specimens[5].

EXPERIMENTAL

Since details of the preparation and fracture of specimens were given previously[5], only an explanatory outline is given here. Notched tensile bars of PMMA, Plexiglas G (Rohm and Haas Co., Philadelphia, Pa., USA) of dimensions $12.7 \times 2.5 \times 0.32$ cm or $12.7 \times 3.2 \times 0.32$ cm, were exposed in air to gamma rays and then stored for up to 6 months in order to remove gaseous products of radiolysis. Because irradiation causes scission with negligible crosslinking of the macromolecules, a unique method of preparation of tensile specimens of low molecular weight results. More conventional methods introduce variables which may produce effects which predominate over effects due to small changes in molecular weight. Viscosity-average molecular weights were calculated from limiting viscosity numbers. The polymers all approximate a random molecular weight distribution for which $\bar{M}_v = 1.9\,\bar{M}_n$, where $\bar{M}_n$ is the number-average molecular weight. Thus another advantage of the preparation of specimens by irradiation is that the average molecular weight can be varied with great precision, while the molecular weight distribution is kept approximately constant.

Specimens were fractured in tension on an Instron machine at a crosshead separation of 0.1 cm/min. As first demonstrated by Zandman[6], certain features of the fracture morphology of PMMA are sensitive to strain rate; however, for the sake of simplicity, this variable is maintained constant in the present work.

Fracture surfaces were examined directly by reflected light with a Zeiss Universal Microscope, Au–Pd was deposited on fracture surfaces examined with an ETEC U-1 Scanning Electron Microscope (SEM) at 5 kV.

RESULTS

Numerous investigators have reported on the fracture morphology of commercially available cast specimens of PMMA, having a $\bar{M}_v > 1 \times 10^6$. However, for completeness and also to clarify the designation of features which have been defined, reference is cited from observations made on a specimen with $\bar{M}_v = 540\,000$ (*Figure 1*). The schematic representation indicates that fracture is initiated at a flaw (F). The crack front first cleaves a relatively smooth 'mirror' region (M) followed by an abrupt transition to a rougher region, described appropriately from examination at low magnification as a 'mist' (S). At higher magnification the mist is seen to include densely packed conical markings, a few of which have been indicated in the schematic. The mist leads into a still rougher region des-

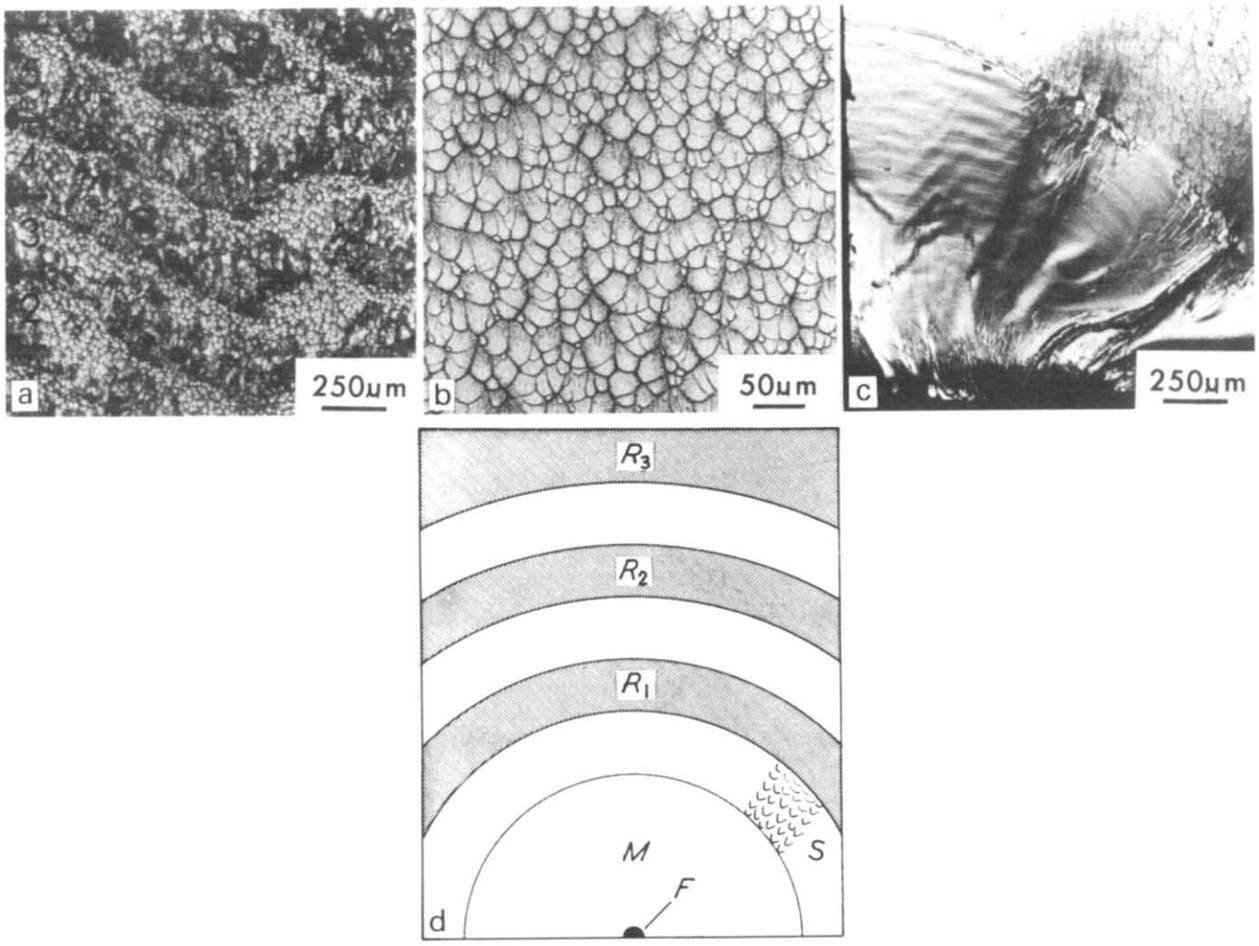

Figure 1 Definition of features of fracture morphology observed for high molecular weight PMMA ($\bar{M}_v$ = 540 000). (a) *R*; (b) *S*; (c) *M*; (d) schematic showing initiation from a centrally situated flaw, but more commonly it is situated at a corner as shown in (c)

cribed as 'hackle' which includes 'ribs' of 'drawn-out material'[1,6] (R_1, R_2, R_3, etc.). In the schematic, the ribs are shown as being regular, but in reality they appear in less orderly patterns and vary in appearance. Actual examples of mirror, mist, and ribs are presented in *Figure 1*. Another feature which is very striking in the mirror region under the light microscope, but which is not apparent in *Figure 1*, is the presence of interference colours. These colours have been investigated in detail and attributed to the presence on the fracture surface of a thin layer of 'crazed' material[7,8]. In addition to the conventional features described above, fine lines can be seen which are more or less symmetrically disposed between the initiating flaw and the boundary of the mirror region. No adequate explanation has been formulated for their appearance.

Examples of the overall change of fracture surfaces with molecular weight down to 85 000 are shown in *Figure 2*. Qualitatively, the findings are consistent with those of Newman and Wolock. The mirror region decreases in area, becoming quite small for $\bar{M}_v$ = 85 000. At molecular weights less than about 60 000, multiple mirrors are often observed indicating that the fracture surface was initiated concurrently from a number of flaws, an effect which might be expected to complicate the surface morphology (cf. *Table 1*). Interference colours were no longer visible in the mirror region in specimens with $\bar{M}_v < 90\,000$.

The mist region also decreases in area with decreasing molecular weight (*Figure 2*), becoming indistinguishable at molecular weights less than about 100 000 (*Table 1*, column 4). A linear fine structure superposed on the parabolic markings was particularly evident in the mist region at $\bar{M}_v \approx 140\,000$ (*Figure 3*). At a molecular weight of 110 000, the mist region included arrays of linear features which also appeared in the hackle region (*Figure 4*).

Details of the morphology of the ribs are revealed at higher magnification of the hackle region (*Figure 5*). Conic markings were seen only at $\bar{M}_v \gtrsim 90\,000$ (*Table 1*, column 5). The rougher portion of these ribs, which includes a lot of 'pulled-out' material (cf. *Figure 5*, areas A and B), is better resolved by SEM (*Figure 6*). The spacing of the ribs is indicated in *Figures 5* and *6*. At the higher molecular weights, rib periodicity may be defined, somewhat arbitrarily, as either the distance between adjacent regions in which conic markings end (often in the form of circular markings, cf. *Figures 1* and *5*) or as the distance between the boundaries of successive smooth and rough regions (the result of crack bifurcation, cf. *Figure 6*). While spacing of these ribs can increase by a factor of as much as three or four with increasing distance from the initiating flaw, this effect is unimportant if attention is confined to the first few fully formed ribs[10]. With this stipulation, ranges of rib spacing were obtained from as many as 10 measurements, the

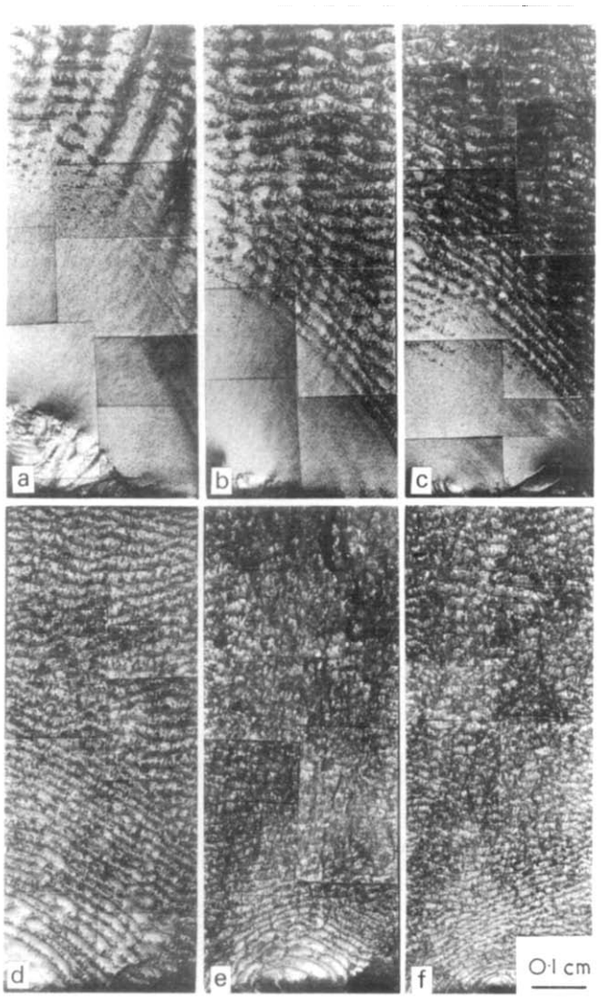

Figure 2 Fracture surfaces for the molecular weight range, $\bar{M}_v$ = 270 000 to 85 000. (a) 270 000; (b) 220 000; (c) 140 000; (d) 110 000; (e) 92 000; (f) 85 000. The prenotched cross-section of each specimen measured 1.1 x 0.3 cm

results of which are shown (*Table 1*, column 6) and a mean value calculated (*Table 1*, column 7). Another notable feature in the hackle region was the appearance of interference colours in the molecular weight range 120 000 to 80 000 (*Table 1*, comments). In the black and white photomicrograph, these coloured regions appear as relatively smooth, lighter patches (cf. *Figure 5*, area C).

At lower molecular weights ($\bar{M}_v$ = 51 000–100 000), the hackle region accounts for the whole fracture surface, apart from a small residual mirror; and the morphology of the ribs is very sensitive to small changes in molecular weight (*Figure 7*). The peculiar mophology of the ribs in a narrow molecular weight region near 69 000 is associated with a new phenomenon: the detachment of a surface film from the mirror region. This phenomenon is exemplified for a specimen of molecular weight 68 000 for which the portion of film detached from one fracture surface can be seen attached to the other (*Figure 8*).

At $\bar{M}_v \simeq 60\,000$ a new feature is visible in the hackle region which appears in optical micrographs as lighter areas. Scanning electron micrographs show that these areas are smooth and without gross structure (*Figure 9*). Recently these features were reported on the surface of a PMMA specimen fractured by cleavage and were termed 'shatter-cones'[4], i.e., percussion fracture cones caused by shock waves. Here the frequency of these brittle features is seen to increase with decreasing molecular weight (cf. *Figure 7*, $\bar{M}_v$ = 55 000 and 51 000). Note, too, the lack of hemispherical shape of the mirror region which often results from the coalescence of multiple mirrors from several fracture initiation sites (*Figure 9a*).

At $\bar{M}_v \lesssim 43\,000$ whole areas of the fracture surface have a glassy featureless appearance. A sequence of surface details illustrating the appearance of the fracture surface, from beginning to end, is given for a specimen of molecular weight 39 000 (*Figure 10*). In frame (a) the mirror region, which has been blown out, is succeeded by a glassy region. This transforms into a region with densely spaced ribs (b)

Table 1 Characterization of fracture morphology of PMMA. ($\bar{M}_v = 5.1 \times 10^4 - 2.7 \times 10^5$)

$\bar{M}_v \times 10^{-5}$	Mirror	Interference colours (mirror)	Mist	Hackle (ribs)	Rib spacing range (μm)	Mean rib spacing (μm)	Comments
2.7	+	r, b	+	+, parabolas	274–289	279	Conventional PMMA failure
2.2	+	r, b	+	+, parabolas	293–315	302	Conventional PMMA failure
1.8	+	r, b	+	+, parabolas	222–282	252	Hackle begins to transform
1.6	+	r, b	+	+, parabolas	224–273	256	Hackle continues to transform
1.4	+	r, b	+	+, parabolas	207–268	233	Hackle continues to transform
1.2	+	r, b	+	+, parabolas	173–234	205	Brilliant patches of colour in hackle region around circular features
1.1	+	?	?	+, parabolas	199–257	230	True mist disappearing
1.0	+	r, b	s	+, parabolas	186–226	204	Brilliant patches of colour persist in hackle region near circular features
0.92	+	?	x	+, parabolas?	110–130	120	Colours in many areas of hackle region
0.85	+	x	x	+, no parabolas	107–133	121	Transformation of hackle region is complete. Occasional dabs of colour in some areas of hackle region
0.79	+	x	x	+, no parabolas	101–108	105	Refinement of ribs continues
0.74	+	x	x	+, no parabolas	79–127	106	Refinement of ribs continues
0.69	+	x	x	+, no parabolas	69–116	92	Refinement of ribs continues
0.65	+	x	x	+, no parabolas	47–75	64	Refinement of ribs continues
0.61	m, s	x	x	+, no parabolas	60–106	84	Refinement of ribs continues
0.58	s	x	x	+, no parabolas	42–49	45	Shatter-cone features begin to appear
0.55	m, s	x	x	+, no parabolas	40–68	55	Frequency of shatter-cone features increases
0.53	m, s	x	x	+, no parabolas	32–57	44	Frequency of shatter-cone features increases
0.51	s	x	x	+, no parabolas	20–24	22	Shatter-cone features intensify

+, observed; ?, questionable; x, not observed; m, multiple; r, red; b, blue; s, small

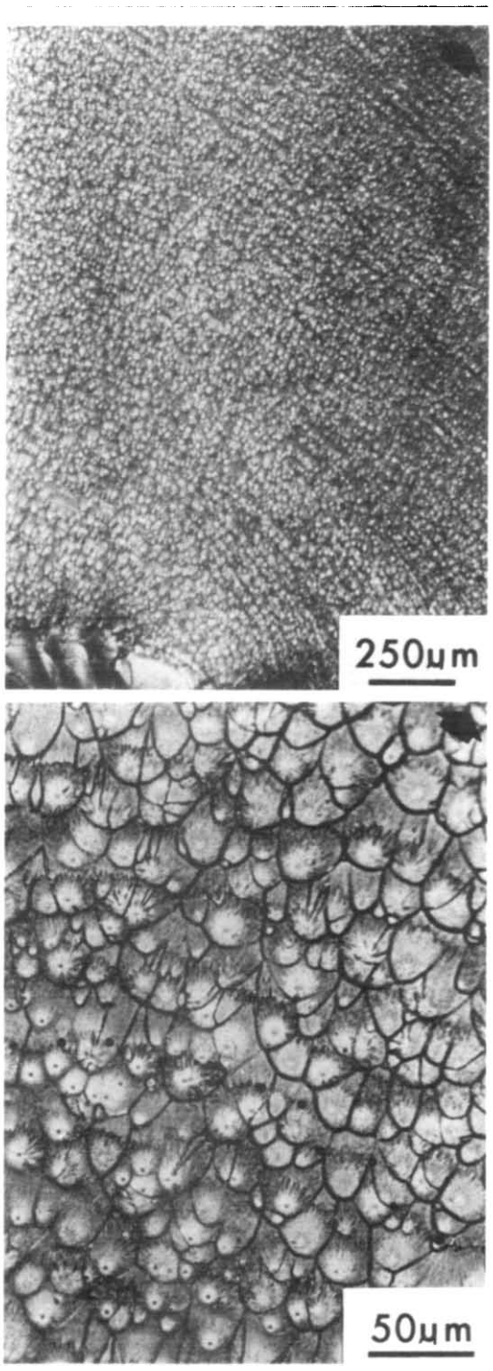

Figure 3 Photomicrographs of linear fine features observed in the mist area (enlarged views of *Figure 2* $\bar{M}_v$ = 140 000). To aid identification, the locus of a single line is represented by a series of superposed dots. Later in the text these features are identified as Wallner lines from a comparison of their geometry with the lines discovered in inorganic glasses[9]. In all Figures the large arrowhead indicates the general direction of crack propagation

marked by progressively increasing areas of shatter-cones (c) until the accumulation of glassy features predominates the fracture topography (d). With decreasing molecular weight, the glassy surface fraction increases as estimated in *Table 2*. Also presented is an overview of other changes which occur over the entire range of molecular weights studied. The scanning electron micrographs of the ribs at $\bar{M}_v$ = 39 000 are shown in *Figure 11*.

As the average molecular chain length becomes still smaller, features which are typical of glassy fracture become even more evident. For a specimen with $\bar{M}_v$ = 28 000 (*Figure 12*), the mottled appearance of the notch at the top of frame (a) precedes the region of crack initiation. Although this region was too irregular to bring into sharp focus in an optical micrograph, nevertheless, a shattered appearance was seen which is common in inorganic glasses. Following a glassy region, irregular zones of lined features (b and c) appear which are formed from intersecting waves (arrowheads). *Figure 12d* is particularly illuminating because two intersecting sets of Wallner lines can be seen clearly in the glassy region. Moreover, individual Wallner lines can be followed out of the glassy region and into the textured region, which on higher magnification resembles the densely packed line system of *Figure 12e*.

Finally at the lowest molecular weight shown (20 000) another characteristic of glassy fracture is seen at an edge of the fracture surface – river patterns (*Figure 13a*). However, even at this molecular weight a fine-lined structure persists on a fraction of the fracture surface (*Figure 13b*). Not until quite low molecular weights does the fine-lined structure, which has been associated with rib periodicity and the hackle region, disappear and a totally glassy surface result (*Table 2*).

DISCUSSION

Fracture morphology is most likely to provide insight into the mechanisms of fracture if studied along with other effects which can be characterized quantitatively. In this direction, renewed efforts have been made along the lines begun by Zandman[6] by attempting to relate fracture morphology to measurements of crack velocity[11–13]. In the present work, initial efforts have concentrated on correlating morphology with measurements of fracture surface energy using specimens covering a wide, yet precisely controlled, range of molecular weights. To put this correlation into perspective, previous data[5] illustrating the dependence of fracture surface energy on molecular weight are shown along with more recent data obtained under slightly different conditions (*Figure 14*). These data indicate that the fracture surface energy really begins to decrease after the $\bar{M}_v$ drops below about 100 000. At the molecular level, a theoretical expression was derived on the simplifying assumption that only molecules above a critical molecular weight could contribute to the predominant term in the fracture surface energy expression, the energy associated with plastic deformation. The best theoretical fit of the experimental data was obtained for the case in which the critical degree of polymerization (x) equalled 1×10^3. The two theoretical curves computed on this basis in *Figure 14* correspond to two types of molecular weight distributions which bracket extremes appropriate for PMMA. The physical basis of the theory is that the plastic contribution to fracture surface energy is controlled by crazing in the vicinity of the crack tip. Moreover, the crazing is dependent on the presence of molecules which are sufficiently long to form an entangled crazed network. At the very lowest molecular weights studied, the fracture surface energy of only several hundred erg/cm^2 corresponded to an almost purely brittle mode of fracture, i.e., with little or no contribution due to plastic deformation.

In agreement with the above view based on considerations of fracture surface energy, the present findings on

Figure 4 Arrays of linear fine features, in the mist (?) and hackle area (enlarged view of *Figure 2*, $\bar{M}_v$ = 110 000). Examples of these arrays are indicated by arrowheads. The nature of these features is unknown. Note also the intersecting bands of parabolas between the mirror region and the first full rib

fracture morphology provide evidence of marked changes by a viscosity-average molecular weight near 100 000. Below this molecular weight, interference colours are no longer observed in the mirror region, the mist region disappears, and conic markings are no longer observed in the hackle region (*Table 1*). From the point of view of correlation with γ, the most important change is the disappearance of interference colours in the mirror region, since previous workers have shown that these colours correspond to the formation of a surface layer which requires a large work of

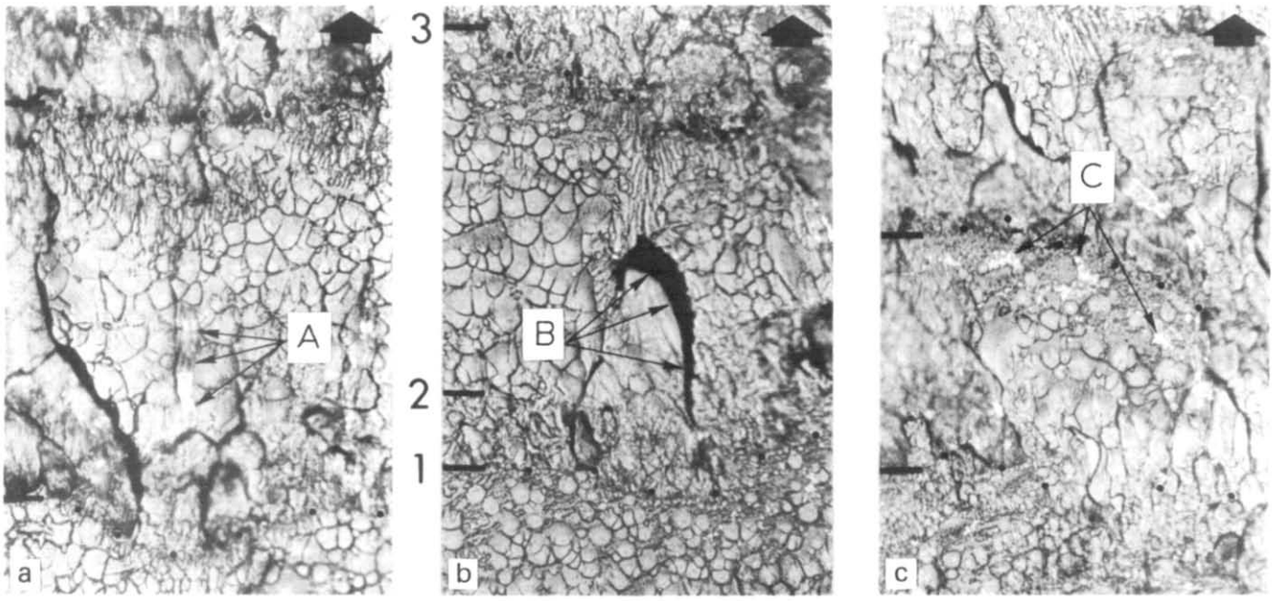

Figure 5 Details of ribs for the molecular weight range 160 000 to 120 000. A and B feature protruding torn-out materials, whereas C indicates regions in which interference colours are observed. The spacing between ribs corresponds to the distance between markers 1 and 3. The rough rib itself is confined mainly between markers 1 and 2. (a) 160 000; (b) 140 000; (c) 120 000

plastic deformation[7,8,14]. While the extent of such work is difficult to estimate, Kambour has made a case that in high molecular weight specimens of PMMA ($\bar{M}_v > 1 \times 10^6$) the work of plastic deformation alone would suffice to account for the fracture surface energy term[8]. As Kambour states 'the strength and ultimate strain of the craze are thus quantities of considerable importance'. Although both these quantities would be expected to decrease with decreasing molecular weight, experimental data are not available to quantitate these factors directly. Consistently, however, below a molecular weight of ~100 000, the craze layer is evidently too thin to produce visible interference effects, while bulk tensile and transverse rupture strengths decrease (cf. *Figure 15*)[15,16].

At lower molecular weights (~68 000), the attachment of the crazed layer to the less deformed polymer becomes sufficiently weak for craze detachment to occur in the mirror region. Craze detachment is quite common in the fracture of polystyrene[17] of high molecular weight but apparently has not been reported for PMMA.

For $\bar{M}_v < 60\,000$ the fracture surface of PMMA becomes increasingly glassy, eventually exhibiting many of the features observed in highly brittle inorganic glasses as summarized, for example, by Smekal[18]. This fracture surface morphology correlates with that previously conjectured on the basis of measurements of fracture surface energies of a few hundred erg/cm^2.

At present the only fracture feature which can be characterized quantitatively over a wide range of molecular weight is the spacing between ribs. However, this involves the implicit assumption that the ribs can be treated as a related group arising from a single mechanism. Now even for high molecular weight specimens, two different classes of mechanisms have been suggested to account for rib formation. Some authors[12], following Andrews[19,20], believe that ribs are related to Wallner lines which are formed by the interaction of the crack tip with states of stress caused by elastic waves generated by fracture[21]. This mechanism has the merit of accounting for ribs with wave-like dispositions and especially for intersecting sets of ribs such as those reported by Andrews in a carbon-filled polyisoprene[19] and in PMMA[20]. On the other hand Benbow has pointed out a serious deficiency of the stress-wave hypothesis, namely that it cannot account for a dependence of rib spacing on molecular weight. The point was that elastic waves are characterized solely by the modulus of elasticity and density but that neither of these quantities is sensitive to molecular weight[22].

The other class of mechanisms suggested to account for rib formation in PMMA of high molecular weight has been designated as 'stick–slip'[20]. Conforming to this description, a recently suggested mechanism[23] may be summarized as follows: 'sticking' occurs after the sudden release of strain energy near the crack tip following the formation of a shower of microcracks which has been observed experimentally. 'Slipping' occurs as the crack tip subsequently follows a craze and then accelerates. Cleavage of crazed material is evidenced by occasional patches exhibiting interference colours (*Figure 5*, area C), while acceleration of the crack tip can be deduced from the change of conic markings from parabolas, through ellipses, and into circles. (For a detailed discussion of this latter argument, made with respect to polystyrene, see ref 24.) Eventually with constantly increasing stress, the strain energy again builds up to some critical value and another rib is initiated by a further shower of microcracks. The general features detailed are similar to those first described by Hull and later by Friedrich on the fracture of polystyrene[25,26].

The present view is that the 'stick–slip' class of mechanism is valid for PMMA in determining the *size* of the rib-spacing. However, the Wallner line phenomenon assumes importance, especially in low molecular weight specimens, by influencing the *disposition* of the ribs. For example, in the intersecting system of Wallner lines visible on the fracture surface of a specimen of molecular weight 28 000 (*Figure 12d*), features are generated which might be regarded as ribs (*Figure 12e*). Similarly in a specimen of $\bar{M}_v$ = 140 000 (*Figure 3*), the fine lines seen in the mist

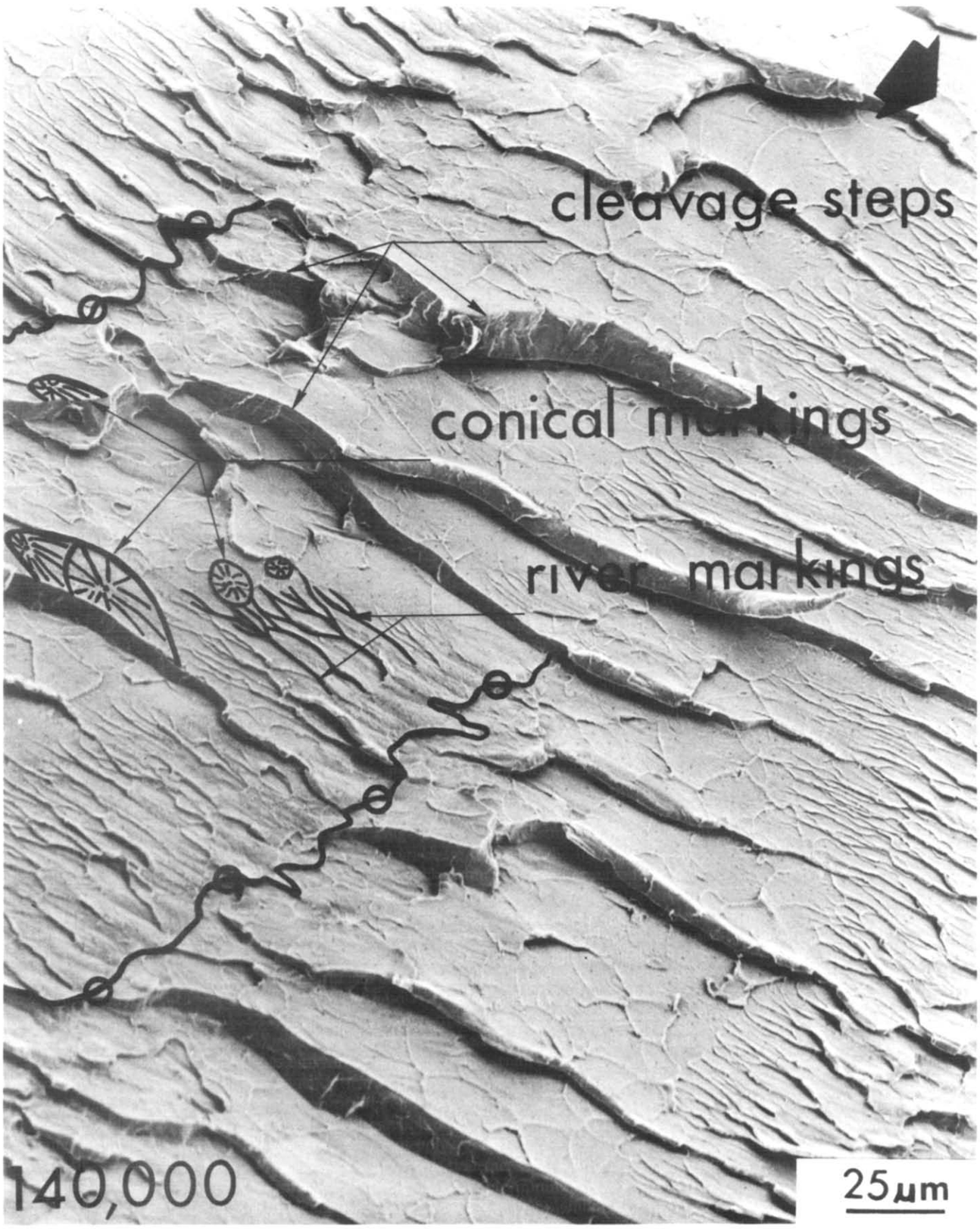

Figure 6 Scanning electron micrograph of rib details. The descriptions used are carried over from metallography. The limits of successive ribs are indicated, in part, by circles joined by irregular lines

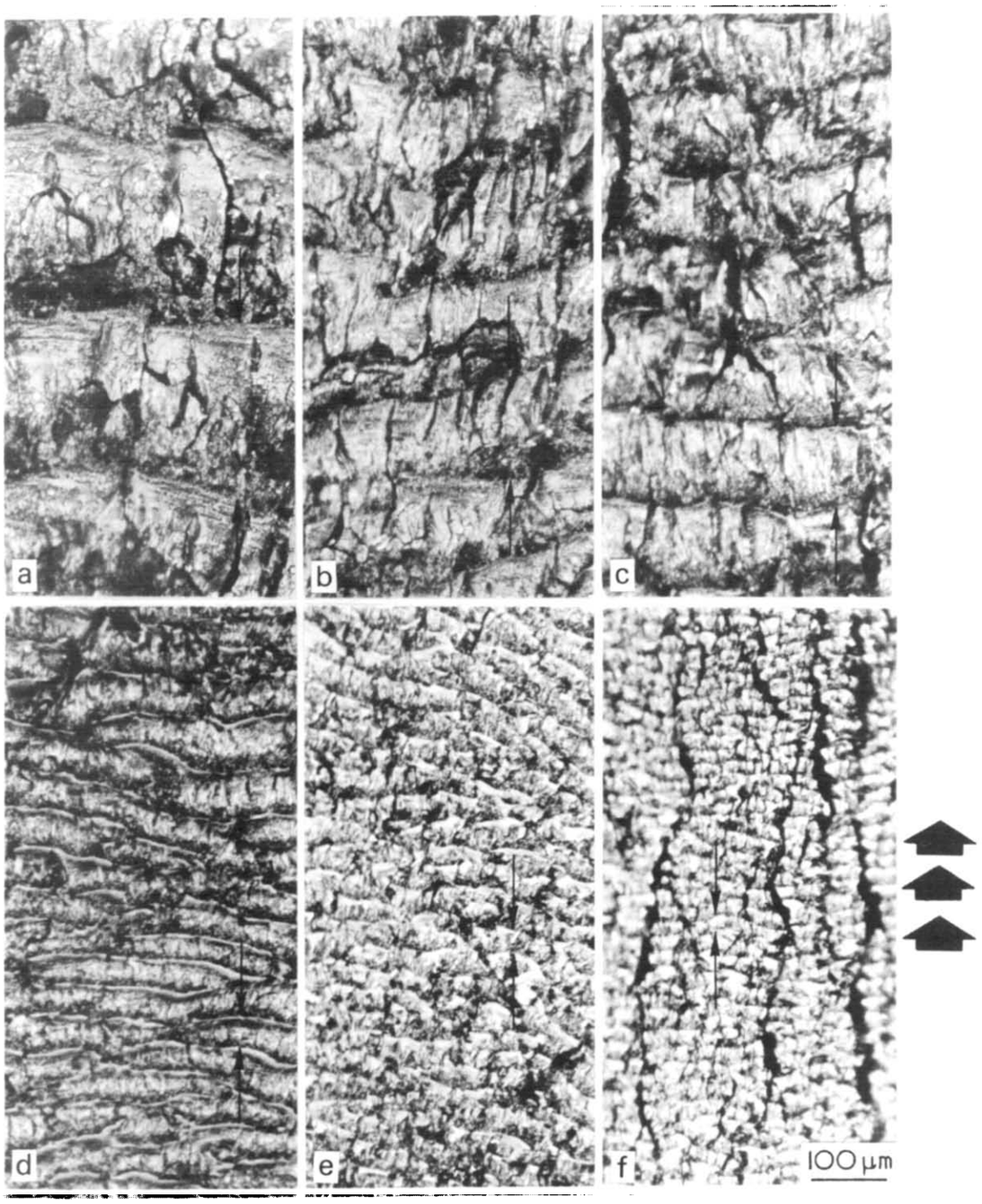

Figure 7 Sensitivity of rib morphology to changes of molecular weight in the range 100 000 to 51 000. (a) 100 000; (b) 92 000; (c) 79 000; (d) 69 000; (e) 55 000; (f) 51 000. For each $\bar{M}_v$ arrowheads bracket one rib spacing

region can be identified as Wallner lines formed by the intersection of the crack front with stress waves emitted from loci along the notch cut (cf. *Figure 2*, 140 000). A detailed account of how such lines are formed may be found in Wallner's paper on inorganic glasses and in the paper by Pratt and Green on PMMA[9,12]. Evidence that the stress waves also influence the disposition of the first few ribs is inferred from their symmetrical relationship to the Wallner lines (cf. *Figure 2*, 140 000). The present view, then, is that stress waves may serve to trigger formation of a shower of microcracks but that the range of this shower and the modulation of the crack within a single craze (if one can indeed form) depends on molecular weight. The molecular weight would be expected to influence both the density of strain energy stored prior to microcracking and also the extent of crazing.

To date the qualitative ideas concerning the dependence of rib spacing (r) on molecular weight ($\bar{M}_v$) have not been cast into a quantitative form. However, attempts have been made to find empirical relationships which might guide further work. While no simple functional relationship has been found between r and $\bar{M}_v$, the plot in *Figure 16* is presented because it serves to summarize results obtained in numerous experiments, including work with cleavage bars, the fabrication of which has been stated elsewhere[27]. Although a linear relationship was obtained using the functions

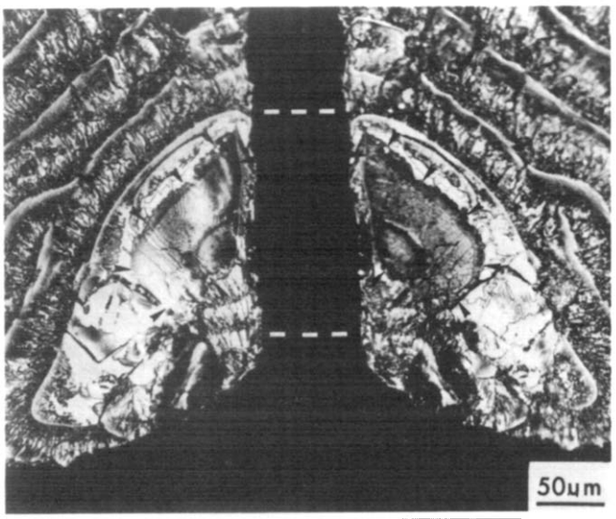

Figure 8 An example of a peculiar rib morphology associated with film detachment in the mirror region. Molecular weight 68 000

Table 2 Overall characterization of fracture morphology of PMMA ($\bar{M}_v$ = 2.6 x 10^3–1.2 x 10^6)

$\bar{M}_v$	Mirror	Interference colours (mirror)	Parabolic markings	Hackle (ribs)	Glassy appearance (%)
1.2 x 10^6	+	+	+	+	0
5.4 x 10^5	+	+	+	+	0
1.2 x 10^5	+	+	+	+	0
6.8 x 10^4	+	?	x	+	0
4.3 x 10^4	+	x	x	+	0
3.9 x 10^4	m	x	x	+	20
2.8 x 10^4	?	x	x	+	30
2.4 x 10^4	x	x	x	+	60
9.5 x 10^3	x	x	x	?	75
6.9 x 10^3	x	x	x	x	95
2.6 x 10^3	x	x	x	x	99

cf. *Table 1*

+, observed; ?, questionable; x, not observed; m, multiple

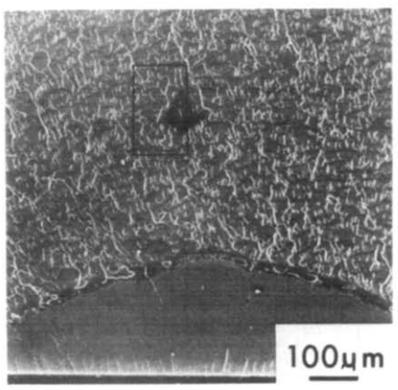

a

b

c

Figure 9 The formation of 'shatter-cones' (M_v = 60 000). Scanning electron micrograph in vicinity of mirror region (a). Comparison of rectangular region by scanning electron (b) and optical (c) microscopy (corresponding points are designated by the crosses). The fiducial hardness mark facilitated fracture relocation

of rib spacing and fracture surface energy shown in *Figure 17*, the significance of this relationship remains to be elucidated. Future work must seek to develop other relations, too, which consider variations in temperature, strain rate, and crosslinking.

CONCLUSIONS

(A) For $\bar{M}_v > 1 \times 10^5$, the fracture morphology of PMMA may be described in conventional terms of mirror, mist, and hackle regions.

At a critical $\bar{M}_v \approx 1 \times 10^5$, significant changes occur on the fracture surface of PMMA. Both the mirror region and the rib spacing in the hackle region decrease in size, while the interference colours, conical features and mist region largely disappear.

As molecular weight gradually decreases to $\bar{M}_v$ = 2600, the fracture assumes a more glassy appearance. While a drastic reduction of rib periodicity occurs, shatter-cone patterns appear with greater frequency. Both river patterns and Wallner lines are evident, too, as the percent of featureless surface increases.

(B) Both stick–slip and Wallner lines play a role in rib formation. The *size* of the rib-spacing is controlled by the former, while the *disposition* of the ribs at low molecular weights is controlled by the latter.

(C) Qualitatively, molecular chain length affects the fracture morphology and physical properties of PMMA. At high molecular weights ($\bar{M}_v > 1 \times 10^5$), the morphology is ductile and rather invariant, while γ is large and relatively constant. In contrast at low molecular weights (e.g. $\bar{M}_v$ = 20 000), the morphology is brittle and γ correspondingly small.

(D) Quantitatively, there does not appear to be a simple relationship between the rib periodicity and molecular chain length, though a linear relationship may exist between the functions γ and r.

ACKNOWLEDGEMENTS

We are grateful to the Applied Radiation Division of NBS and the Physics Department at UNC for use of the ^{60}Co

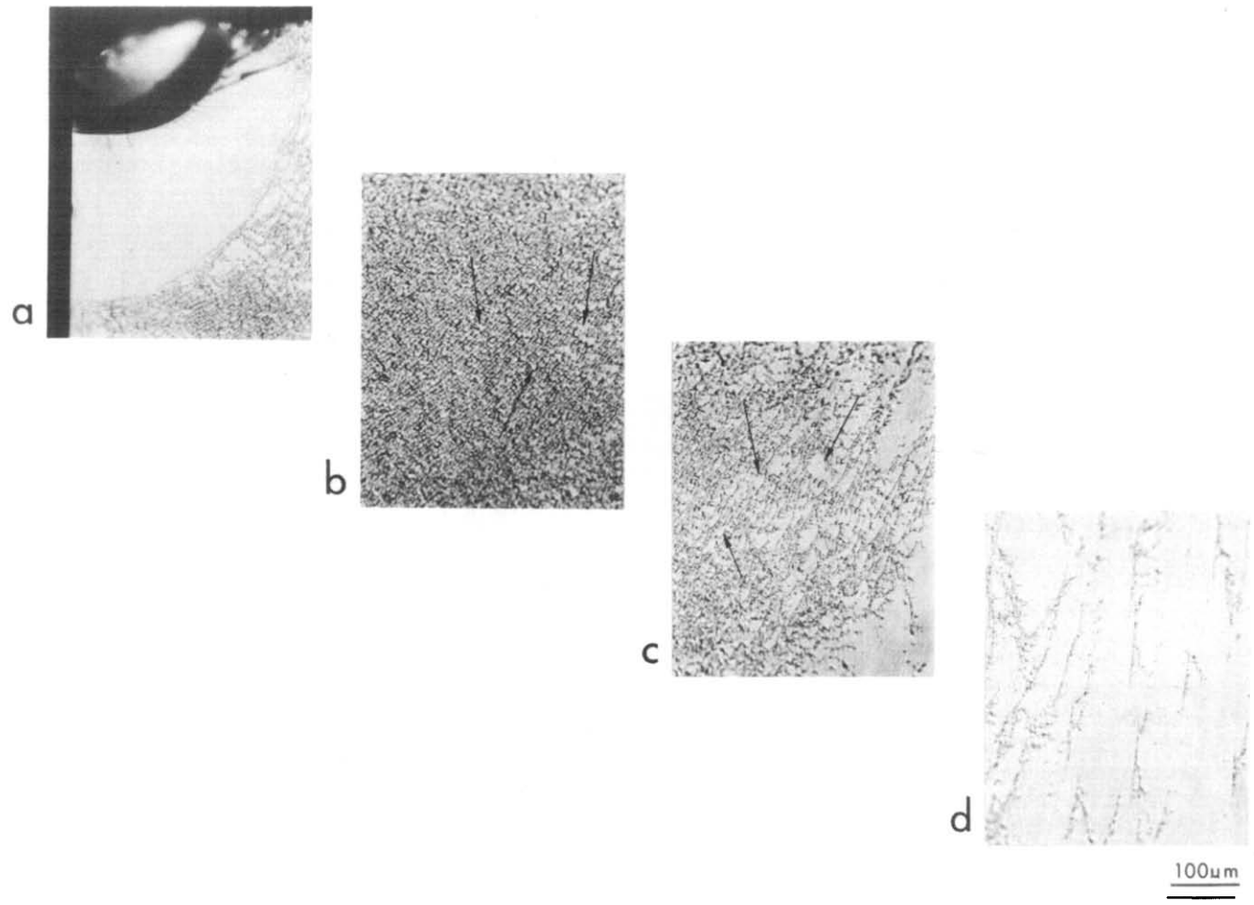

Figure 10 Overall view of fracture surface in the molecular weight range where glassy fracture becomes significant (cf. *Table 2*) (M_v = 39 000). The fracture surface is traversed from beginning to end in the sequence a to d. The arrowheads indicate shatter-cone features

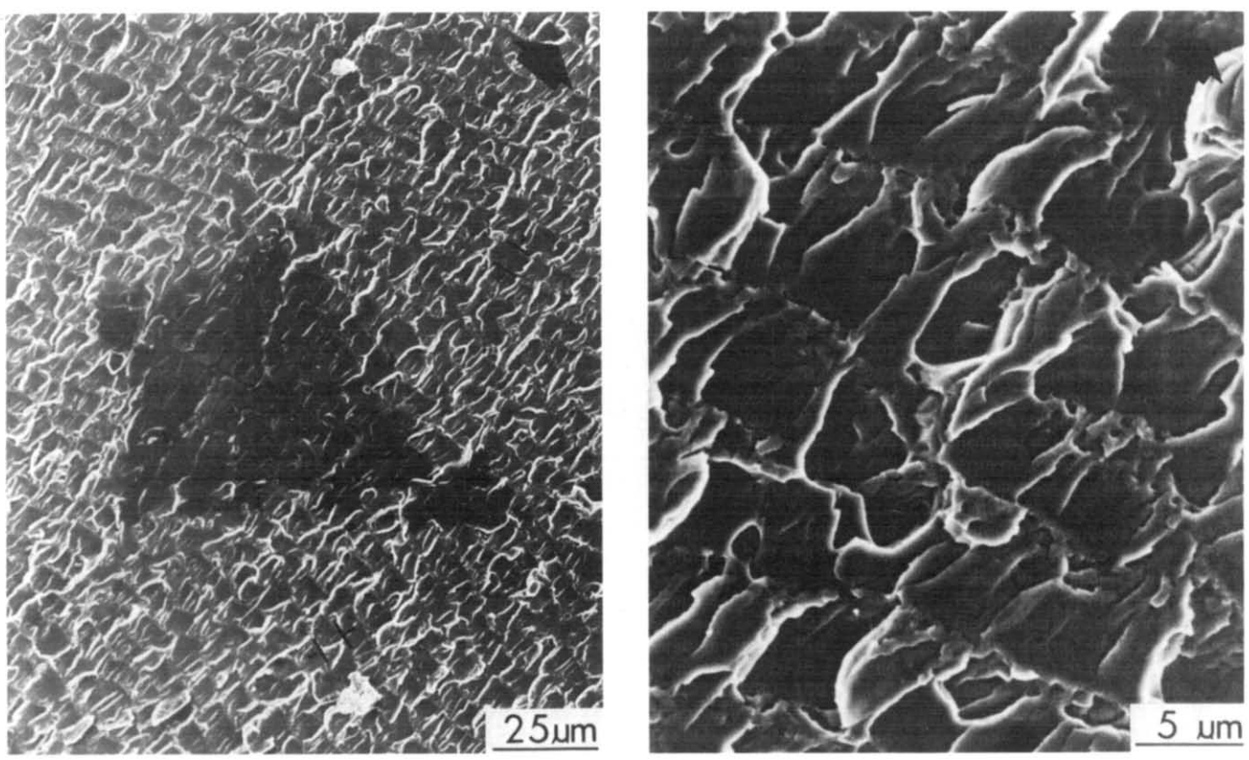

Figure 11 Appearance of ribs at $\bar{M}_v$ = 39 000 (SEM). The definition of rib spacings is indicated by brackets at the lower magnification. At the higher magnification, the boundaries of a rib are indicated by the broken lines. Note the delicate lacelike features, consistent with the lower magnitude of γ

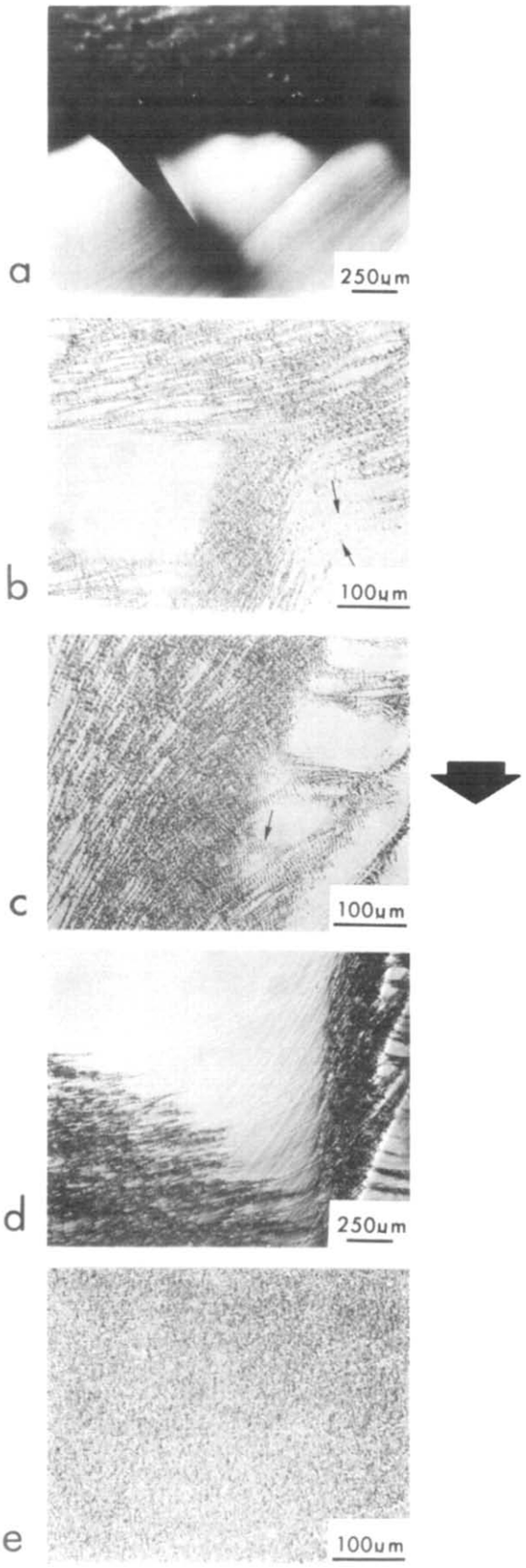

Figure 12 Relationship between Wallner lines and the darker line features ($\bar{M}_v$ = 28 000). The fracture surface is traversed from beginning to end in the sequence a to e. Arrowheads suggest additional features formed by intersecting Wallner lines

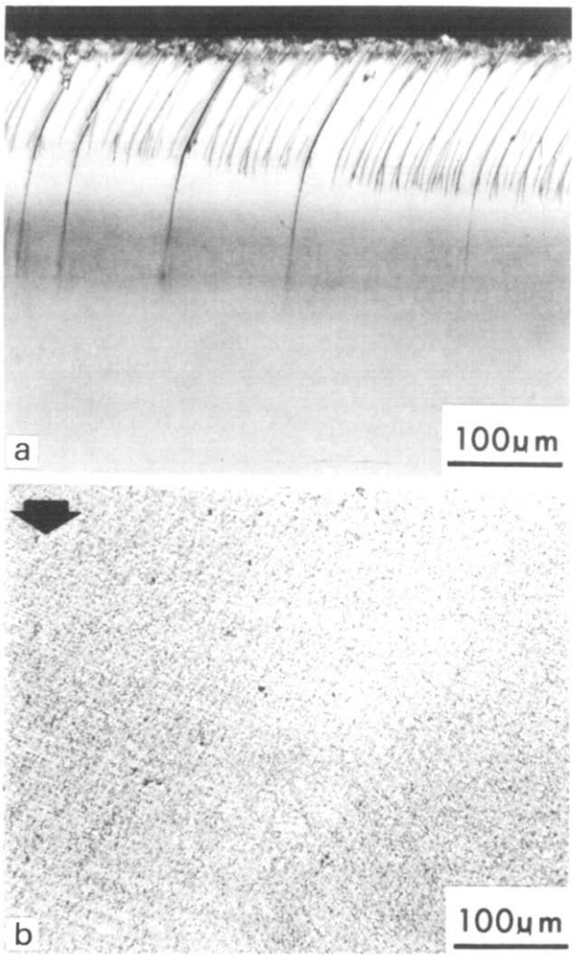

Figure 13 Relatively featureless fracture surface at $\bar{M}_v$ = 20 000. Two-thirds of this fracture surface is glassy (cf. *Table 2*) (a), while the balance has fine lines (b)

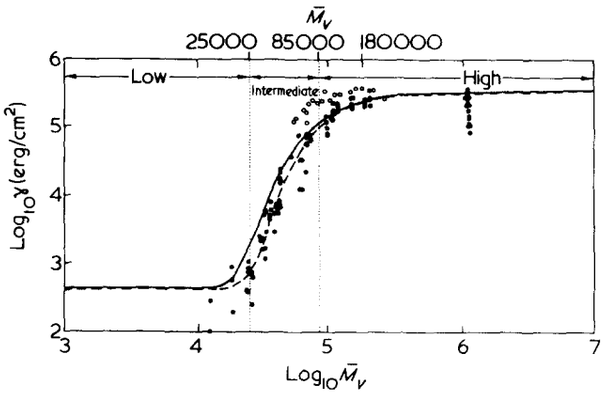

Figure 14 Relationship between fracture surface energy and molecular weight. —— and –·–·–, were calculated for k = 1 and k = 2, respectively, when the critical number of monomer units required for plastic deformation (x) equalled 1 x 10^3 (cf. ref 5). ●, represent notched tensile bars previously described (ref 5); ○, represent notched tensile bars characterized in *Table 1*. Measuring 1.1 x 0.3 cm in cross-section and 5.0 cm long, these bars were fractured at a crosshead separation of 0.1 cm/min

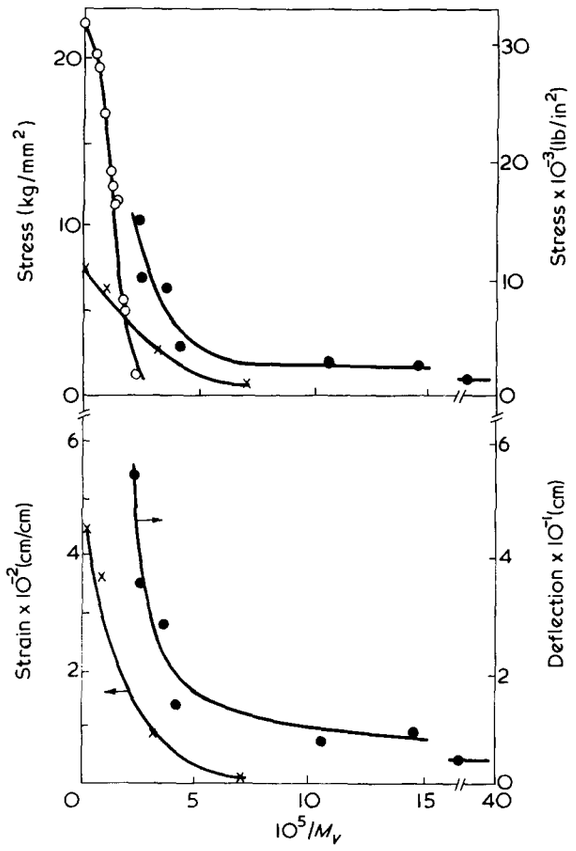

Figure 15 Plot of ultimate stress and strain *versus* reciprocal molecular weight in bulk PMMA, ●, Present work, mean flexural strength and deflection at 22°C (see testing procedure, ref 5); ○, Vincent, flexural strength at −196°C (ref 16); x, Bopp and Sisman, tensile strength and strain at 22°C (ref 15).

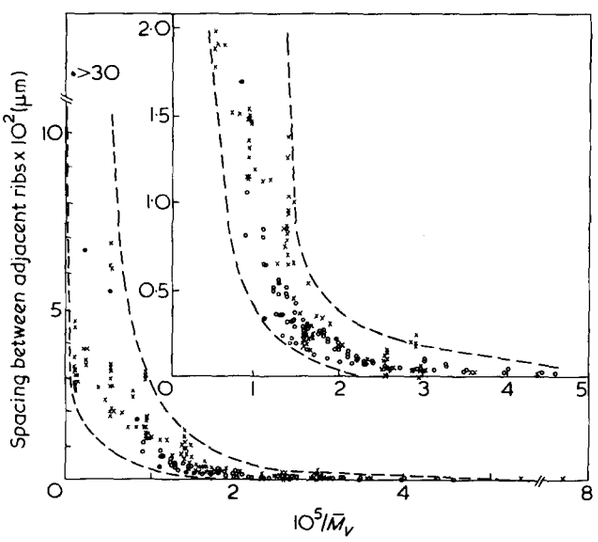

Figure 16 Plot of rib spacing *versus* reciprocal molecular weight. ●, Newman and Wolock; ○, present work (cleavage); x, present work (tension)

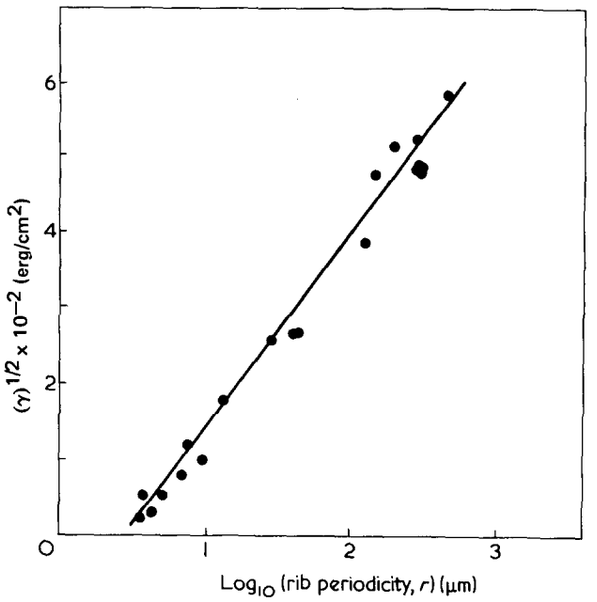

Figure 17 Empirical plot of functions of fracture surface energy (γ) and rib periodicity (spacing) (r)

and ^{137}Cs facilities. This investigation was supported by NIH research grant number DE 02668 from the National Institute of Dental Research and by NIH grant number RR 05333 from the Division of Research Facilities and Resources.

REFERENCES

1 Newman, S. B. and Wolock, I. *J. Appl. Phys.* 1958, **29**, 49
2 Busse, W. F., Orowan, E. and Niemark, J. E. *Am. Phys. Soc. Philadelphia, Pa., USA* March 1957
3 Higuchi, M. Rep. *Res. Inst. Appl. Mech. Kyushu Univ.* 1958, **6**, 173
4 Kusy, R. P. *J. Mater. Sci.* 1976, **11**, 1381
5 Kusy, R. P. and Turner, D. T. *Polymer* 1976, **17**, 161
6 Zandman, F. 'Etudes de la Déformation et de la Rupture des Matières Plastiques', Publications Scientifiques et Techniques de Ministère de l'Air, Paris, 1954
7 Berry, J. P. *J. Polym. Sci.* 1861, **50**, 107, 313
8 Kambour, R. P. *Appl. Polym. Symp.* 1968, **7**, 215
9 Wallner, H. *Z. Phys.* 1939, **114**, 368
10 Kusy, R. P., Lee, H. B. and Turner, D. T. unpublished work
11 Kobayashi, A., Ohtani, N. and Sato, T. *J. Appl. Polym. Sci.* 1974, **18**, 1625
12 Green, A. K. and Pratt, P. L. *Eng. Fract. Mech.* 1974, **6**, 71
13 Döll, W. *J. Mater. Sci.* 1975, **10**, 935
14 Lednicky, F. and Pelzbauer, Z. *J. Polym. Sci. (C)* 1972, **38**, 375
15 Bopp, C. D. and Sisman, O. *Nucleonics* 1955, **13**, 28
16 Vincent, P. I. *Polymer* 1960, **1**, 425
17 Newman, S. B. *Polym. Eng. Sci.* 1965, **5**, 159
18 Smekal, A. *Ergeb. Exakt. Naturwiss.* 1936, **15**, 106
19 Andrews, E. H. *J. Appl. Phys.* 1959, **30**, 740
20 Andrews, E. H. 'Fracture in Polymers', Elsevier, New York, 1968, Ch 6
21 Guz, I. S. and Finkel, V. M. *Sov. Phys. Solid State* 1973, **14**, 1619
22 Benbow, J. J. *Proc. Phys. Soc.* 1961, **78**, 970
23 Kusy, R. P., Lee, H. B. and Turner, D. T. *J. Mater. Sci.* 1976, **11**, 118
24 Doyle, M. A., Mancini, A., Orowan, E. and Stork, S. T. *Proc. Roy. Soc. (A)* 1972, **329**, 137
25 Hull, D. *J. Mater. Sci.* 1970, **5**, 357
26 Friedrich, K. *Prakt. Metallogr.* 1975, **12**, 587
27 Kusy, R. P. and Katz, M. J. *J. Mater. Sci.* 1976, **11**, 1475